9580

NACA TN 3289

TECH LIBRARY KAFB, NM
0066235

NATIONAL ADVISORY COMMITTEE FOR AERONAUTICS

TECHNICAL NOTE 3289

THE MINIMIZATION OF WAVE DRAG FOR WINGS AND BODIES WITH GIVEN BASE AREA OR VOLUME

By Max. A. Heaslet

Ames Aeronautical Laboratory
Moffett Field, Calif.

Washington
July 1957

AFMDC
TECH

TECH LIBRARY KAFB, NM
0066235

.U

NATIONAL ADVISORY COMMITTEE FOR AERONAUTI

TECHNICAL NOTE 3289

THE MINIMIZATION OF WAVE DRAG FOR WINGS AND BODIES WITH GIVEN BASE AREA OR VOLUME

By Max. A. Heaslet

SUMMARY

The minimization of wave drag for thin aerodynamic shapes carrying no lift is studied for conditions under which either base area or volume is specified. When volume alone is given, the analysis is limited to shapes with straight trailing edges normal to the stream direction. The problem of minimization is reduced to one of finding a two-dimensional harmonic function with known boundary conditions.

In several examples the theory is applied to the calculation of minimum drag. For given base area, general formulas are found that cover as special cases quasi-cylindrical bodies of revolution, wings having plan forms with fore and aft symmetry, slender bodies, and certain classes of yawed wings. The drag can in fact be determined from a unidimensional flow analysis in a duct of known shape. For given volume, minimization of the external wave drag of a ducted body of revolution of arbitrary radius is achieved in closed analytic form.

In two cases, the determination of surface shape corresponding to the minimum drag is carried to completion.

INTRODUCTION

To seek conditions under which the wave drag of a given wing or body is minimized is to seek conditions for economical supersonic flight. It is also a common experience, in the study of such problems, to find that a gratuitous economy appears to affect the analysis itself. Almost invariably, simplicity characterizes the final forms of the results in comparison with predictions carried out for wings and bodies chosen with less discrimination. In the present paper, the minimization of wave drag for aerodynamic shapes carrying no lift is studied. Conditions must, of course, be fixed in order to prescribe the problem and, from a practical point of view, this choice is less obvious than in studies of lifting configurations where a given weight is to be supported aerodynamically. The cases treated here apply the conventional constraints on base area and enclosed volume to a variety of shapes. For a large class of wings and bodies, the above-mentioned simplicity is especially apparent in the case of given base area for, as will be shown, the general expression

for minimum drag assumes the most elementary form possible while at the same time retaining the relevant parameters and being dimensionally correct.

The starting point of the present work is the expression for drag given by G. N. Ward (ref. 1) in his study of thin lifting bodies, that is, wings and bodies for which linearized supersonic flow theory applies. The body shape is assumed to be enclosed by a characteristic surface generated as the envelope of both the downstream-facing Mach cones, with vertices on the forward edge of the body, and the upstream-facing Mach cones, with vertices on the trailing edge of the body. Wave drag (plus vortex drag when lift is present) is then given by a control-surface integral of the induced velocities over the downstream portion of the Mach envelope. This particular control surface has analytical advantages similar to those exploited by R. T. Jones (refs. 2 and 3) in the use of combined flow fields. Jones adopts a perturbation potential equal to the sum of the potentials in forward and reverse flow. He then shows, for example, that the necessary condition for minimum wave drag is, for a plan form of given base area, that the pressure in the combined flow field be a constant over the plan form. It follows that locally the combined-flow potential is a two-dimensional harmonic function. If, however, the entire analysis is committed to the use of combined flows, details of body shape (or, in the lifting case, surface loading) are lost. Along the Mach envelope used by Ward the perturbation potential in forward flow is equal in magnitude to its value in the combined flow field. Drag minimization then determines conditions on the control surface and for the problem of given base area the potential on the surface differs from a harmonic function by a known amount. The conventional perturbation potential is retained but the determination of the body shape is still not direct. Mathematically, one needs to invert an integral equation and the question as to uniqueness of solution arises. The final examples in the present paper will be concerned with the construction of minimum-drag bodies of revolution from the known conditions on the control surface. In these special cases the inversions of the integral equations are easily carried out.

ANALYSIS

The following analysis is divided into two sections. First, integral relations are derived that determine the drag, base area, and volume of a thin body in terms of induced velocities on the rear Mach envelope. Second, variational methods are applied so as to minimize wave drag subject to the imposed constraints. The perturbation potential on the Mach envelope is in this way related to a two-dimensional harmonic function satisfying known boundary conditions.

Relations for Drag, Base Area, and Volume

It is assumed that the given body deviates slightly from a planar or a cylindrical reference surface with elements passing through the leading edge of the body and extending back parallel to the stream direction. As shown in sketch (a), the body reference surface is denoted Σ_0, the over-all length is l, and a Cartesian coordinate system is to be used with the origin fixed at the foremost point of the body and the x axis alined with the free-stream direction. The constant free-stream velocity, Mach number, and density are U_∞, M_∞, and ρ_∞, respectively. The perturbation velocity components u, v, w induced by the body in the x, y, z directions are given by the gradients of the perturbation velocity potential $\varphi(x,y,z)$, that is, by $\varphi_x(x,y,z)$, $\varphi_y(x,y,z)$, $\varphi_z(x,y,z)$. Since supersonic small-disturbance theory is assumed to apply, the flow field is governed by the linearized differential equation

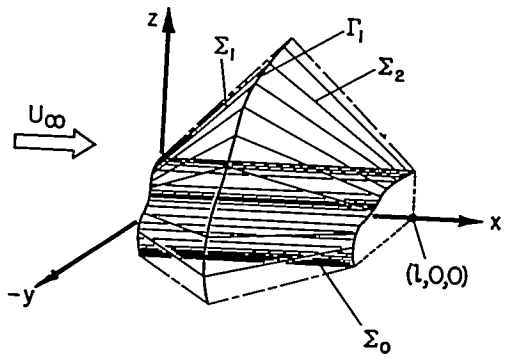

Sketch (a)

$$\beta^2\varphi_{xx} - \varphi_{yy} - \varphi_{zz} = 0 \tag{1}$$

where $\beta^2 = M_\infty^2 - 1$.

Three types of reference surfaces occur most often in practice: first, planes which are associated with the study of wings; second, circular cylinders which lead to the study of internal or external flow around quasi-cylindrical bodies; third, lines parallel to the stream direction. The last case is associated with slender-body theory and is merely a limiting form of the previous cases. The thickness distribution of the wing or body is fixed by boundary conditions prescribed on the reference surface. In order to avoid difficulties concerning gaps or holes in the body surface it will be assumed that unique leading and trailing edges exist and that the thickness distribution does not vanish between these extremities.

In sketch (a) the characteristic surfaces enclosing the body are indicated. The front portion, Σ_1, is the envelope of the Mach cones stemming back from the leading edge of the body and the rear portion, Σ_2, is the envelope of the Mach cones facing forward from the trailing edge. The surfaces Σ_1 and Σ_2 intersect along the space curve Γ_1. As shown by Ward (ref. 1), the wave drag can be expressed in terms of an integral over the surface Σ_2. This follows from an application of momentum principles to the three-dimensional region bounded by Σ_0, Σ_1, and Σ_2. The force on the body is expressed vectorially in the form (see, e.g., ref. 4, p. 222)

$$\vec{F} = -\iint_{\Sigma} (p-p_\infty)d\vec{\Sigma} - \iint_{\Sigma} \rho\vec{V}\left[\left(\vec{U}_\infty+\vec{V}\right)\cdot d\vec{\Sigma}\right]$$

where the subscript ∞ denotes free-stream conditions, p and ρ are local static pressure and density, $\vec{V}$ is the local perturbation velocity vector, and the surface integrations extend over the bounding surfaces. In small-disturbance theory the approximate relations

$$\rho/\rho_\infty = 1 - M_\infty{}^2(u/U_\infty)$$

and

$$p-p_\infty = -\rho_\infty\left[U_\infty u + \frac{1}{2}\left(-\beta^2u^2+v^2+w^2\right)\right]$$

may be used.

If $\cos(\nu,x)$, $\cos(\nu,y)$, $\cos(\nu,z)$ are the direction cosines of the inner normal ν to the enclosing surface, drag (wave plus vortex drag) is, to the order of the approximations,

$$D = -\frac{\rho_\infty}{2}\iint_{\Sigma_2}\left\{(v^2+w^2) + u\left[\beta^2u-2v\frac{\cos(\nu,y)}{\cos(\nu,x)} -2w\frac{\cos(\nu,z)}{\cos(\nu,x)}\right]\right\}\cos(\nu,x)d\Sigma \tag{2}$$

An essential simplification of the drag formula follows if one introduces the function $\chi(y,z)$ where

$$\chi = \varphi[f(y,z),y,z]$$

and $x = f(y,z)$ is the equation of the characteristic surface Σ_2. The function χ is thus the value of the perturbation potential on Σ_2. The direction numbers of the normal on this surface are given by

$$\cos(\nu,x):\cos(\nu,y):\cos(\nu,z) = -1:f_y:f_z \tag{3}$$

and the relation

$$f_y{}^2 + f_z{}^2 = \beta^2$$

holds. Since

$$\chi_y = v + uf_y \qquad \chi_z = w + uf_z$$

the drag formula becomes

$$D = -\frac{\rho_\infty}{2}\iint_{\Sigma_2}(\chi_y{}^2 + \chi_z{}^2)\cos(\nu,x)\,d\Sigma \tag{4a}$$

$$= -\frac{\rho_\infty}{2}\iint_{S}\chi\nabla^2\chi\,dy\,dz - \frac{\rho_\infty}{2}\int_{C_2}\chi\frac{\partial}{\partial n}\chi\,ds \tag{4b}$$

The latter relation is a direct consequence of Green's theorem in the two-dimensional cross-plane; ∇^2 is the Laplacian operator $(\partial^2/\partial y^2)+(\partial^2/\partial z^2)$ and n is the inner normal to the boundary curves in the yz plane. As indicated in sketch (b), the integration in equation (4b) extends over the area S which is the projection of Σ_2 on the plane $x = \text{const}$. Along the outer curve C_1, which is the trace of the curve Γ_1 in the same plane, the function χ vanishes since Γ_1 also lies on the Mach cones from the leading edge. The inner curve C_2 is the trace of the cylindrical reference surface.

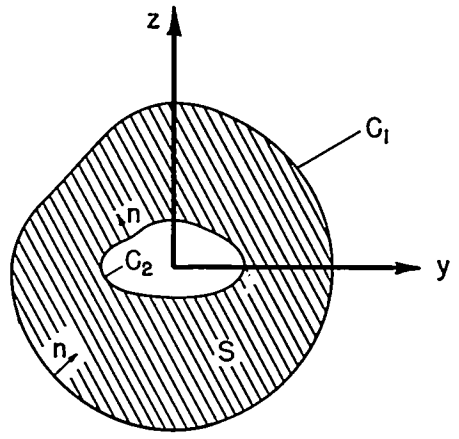

Sketch (b)

In order to evaluate the base area external to the reference surface Σ_0, it is sufficient to apply over the surfaces Σ_0, Σ_1, and Σ_2 the first-order form of the integral expression for continuity of mass flow. This conservation relation is, for compressible flow,

$$\iint_{\Sigma}\rho\frac{\partial}{\partial\nu}(U_\infty x + \varphi)\,d\Sigma = 0$$

and to the order of the present linearized analysis becomes

$$\rho_\infty U_\infty\iint_{\Sigma_0}\frac{1}{U_\infty}\frac{\partial\varphi}{\partial\nu}\,d\Sigma + \rho_\infty U_\infty\iint_{\Sigma_2}\left[-\beta^2\frac{u}{U_\infty} + \frac{v}{U_\infty}\frac{\cos(\nu,y)}{\cos(\nu,x)} + \frac{w}{U_\infty}\frac{\cos(\nu,z)}{\cos(\nu,x)}\right]\cos(\nu,x)\,d\Sigma = 0$$

where the two integrations extend, as indicated, over Σ_0 and the rear Mach envelope Σ_2, respectively. In linear theory the term $(1/U_\infty)(\partial\varphi/\partial\nu)$, appearing as the first integrand, is equal to the slope, relative to the stream direction, of the body surface. The x-wise integration of the first integral thus yields the difference in body ordinates at the trailing and leading edges and the complete integration can then be written

$$\rho_\infty U_\infty \iint_{\Sigma_0} \frac{1}{U_\infty} \frac{\partial\varphi}{\partial\nu}\, dx\, dy = \rho_\infty U_\infty A$$

where A is the increment of area between the nose and tail of the body. In the notation of equations (3) and (4), continuity of mass flow thus leads to the desired relations

$$A = -\frac{1}{U_\infty}\iint_S (\chi_y f_y + \chi_z f_z)\, dy\, dz \tag{5a}$$

$$= \frac{1}{U_\infty}\iint_S \chi\nabla^2 f\, dy\, dz + \frac{1}{U_\infty}\int_{C_2} \chi \frac{\partial f}{\partial n}\, ds \tag{5b}$$

It remains to determine an analogous expression for the volume V between Σ_0 and the body itself. The starting relation is Green's theorem written in the form

$$\iiint_\tau \rho(U_\infty + u)\, dx\, dy\, dz$$

$$= -\iint_\Sigma \rho x \frac{\partial}{\partial\nu}(U_\infty x + \varphi)\, d\Sigma - \iiint_\tau x\left\{\frac{\partial}{\partial x}\left[\rho(U_\infty + \varphi_x)\right] + \frac{\partial}{\partial y}(\rho\varphi_y) + \frac{\partial}{\partial z}(\rho\varphi_z)\right\} dx\, dy\, dz$$

where τ is the three-dimensional region enclosed by the surfaces Σ_0, Σ_1, and Σ_2. The factor within the braces, in the final term, is, however, zero throughout the region for steady-state, continuous, compressible flow conditions. To first order, the relation becomes

$$\iiint_\tau \beta^2 u\, dx\, dy\, dz$$

$$= \iint_{\Sigma_0} x \frac{\partial\varphi}{\partial\nu}\, d\Sigma + \iint_{\Sigma_2}\left[-\beta^2 u + v\frac{\cos(\nu,y)}{\cos(\nu,x)} + w\frac{\cos(\nu,z)}{\cos(\nu,x)}\right] x \cos(\nu,x)\, d\Sigma$$

If, in the first term, the x-wise integration is performed and, in the second term, the boundary conditions on Σ_0 are introduced and an x-wise integration by parts is carried out, one then gets

$$\beta^2\iint_S \chi\, dy\, dz = U_\infty\int_{C_2} fN(f,s)\, ds - U_\infty V + \iint_S f(\chi_y f_y + \chi_z f_z)\, dy\, dz$$

where $N = N(x,s)$ is a measure of the deviation of the body from the control surface, that is, the distance measured normal to Σ_0 between Σ_0 and the body. Thus $N = N(f,s)$ is the deviation of the body from the control surface at the base. From Green's theorem, the last term is

$$\iint_S f(\chi_y f_y + \chi_z f_z)\,dy\,dz = -\frac{1}{2}\iint_S \chi\nabla^2 f^2\,dy\,dz - \frac{1}{2}\int_{C_2} \chi\,\frac{\partial f^2}{\partial n}\,ds$$

and the volume formula becomes

$$V = \int_{C_2} fN(f,s)\,ds - \frac{1}{2U_\infty}\iint_S \chi\nabla^2\left[f^2 + \frac{1}{2}\beta^2(y^2+z^2)\right]dy\,dz - \frac{1}{2U_\infty}\int_{C_2} \chi\,\frac{\partial f^2}{\partial n}\,ds \tag{6}$$

Further simplification of equation (6) occurs if the trailing edge of the body lies in a plane perpendicular to the x axis. The first integral in the right member then becomes l times base area where l is body length and the term can then be re-expressed by means of equation (5b). For trailing edges normal to the stream, volume then becomes

$$V = -\frac{1}{2U_\infty}\iint_S \chi\nabla^2\left[(l-f)^2 + \frac{1}{2}\beta^2(y^2+z^2)\right]dy\,dz - \frac{1}{2U_\infty}\int_{C_2} \chi\,\frac{\partial}{\partial n}(l-f)^2\,ds \tag{7}$$

Solution of Variational Problem

By means of the previous relations, wave drag can be minimized for prescribed values of incremental base area, A, and volume, V, external to Σ_0. Since equation (7) is to be used, results involving volume V will be applicable only to configurations with trailing edges normal to the stream direction but this restriction need not be invoked when conditions are prescribed solely for the area A. The formal solution of this isoperimetric problem is achieved through the minimization of the expression

$$I = D - \lambda A + \mu V \tag{8}$$

where D, A, and V are given, respectively, by equations (4b), (5b), and (7) and λ,μ are Lagrangian multipliers. Let χ be replaced by $\chi + \alpha\eta(y,z)$ where $\eta(y,z)$ represents a variation that satisfies the same boundary conditions as χ on C_1 and C_2 and α is a constant. The necessary condition for minimization is that the expression

$$\iint_S \eta\nabla^2\left\{\chi + \frac{\lambda}{\rho_\infty U_\infty} f + \frac{\mu}{2\rho_\infty U_\infty}\left[(l-f)^2 + \frac{1}{2}\beta^2(y^2+z^2)\right]\right\} dy\, dz +$$

$$\int_{C_2} \eta \frac{\partial}{\partial n}\left[\chi + \frac{\lambda}{\rho_\infty U_\infty} f + \frac{\mu}{2\rho_\infty U_\infty}(l-f)^2\right] ds = 0$$

holds for all η. The following differential equation and boundary conditions must therefore be satisfied

$$\left.\begin{aligned}
&\nabla^2\left\{\chi + \frac{\lambda}{\rho_\infty U_\infty} f + \frac{\mu}{2\rho_\infty U_\infty}\left[(l-f)^2 + \frac{1}{2}\beta^2(y^2+z^2)\right]\right\} = 0 \quad \text{in } S \\
&\frac{\partial}{\partial n}\left[\chi + \frac{\lambda}{\rho_\infty U_\infty} f + \frac{\mu}{2\rho_\infty U_\infty}(l-f)^2\right] = 0 \quad \text{on } C_2 \\
&\chi = 0 \quad \text{on } C_1
\end{aligned}\right\} \tag{9}$$

Equations (9) are closely analogous to conditions arising in the minimization of wave plus vortex drag for wings having given lift and given center of pressure. It should be remarked that the particular form of the term involving $(y^2 + z^2)$ in the bracketed term of the harmonic differential equation is somewhat arbitrary and that, for example, the equation could be changed to one of the Poisson type with the term in question appearing in the right member as a constant times the Lagrangian multiplier μ.

For purposes of direct solution it is sometimes preferable to introduce the function $\Omega(y,z)$ in equation (9) where

$$\Omega(y,z) = \chi + \frac{\lambda}{\rho_\infty U_\infty} f + \frac{\mu}{2\rho_\infty U_\infty}\left[(l-f)^2 + \frac{1}{2}\beta^2(y^2+z^2)\right] \tag{10}$$

The equations to be solved are, then,

$$\left.\begin{aligned} &\nabla^2\Omega = 0 \quad \text{in } S \\ &\frac{\partial}{\partial n}\Omega = \frac{\mu\beta^2}{4\rho_\infty U_\infty}\frac{\partial}{\partial n}(y^2+z^2) \quad \text{on } C_2 \\ &\Omega = \frac{\lambda}{\rho_\infty U_\infty} f + \frac{\mu}{2\rho_\infty U_\infty}\left[(l-f)^2 + \frac{1}{2}\beta^2(y^2+z^2)\right] \quad \text{on } C_1 \end{aligned}\right\} \tag{11}$$

The function χ thus differs from the harmonic function Ω by an amount given explicitly in terms of the characteristic surface Σ_2.

An important expression for the wave drag can be derived from equations (9) without further knowledge of the solution. For, from equations (4b) and (9), one has

$$D = \frac{\rho_\infty}{2}\iint_S \chi\nabla^2\left\{\frac{\lambda}{\rho_\infty U_\infty} f + \frac{\mu}{2\rho_\infty U_\infty}\left[(l-f)^2 + \frac{1}{2}\beta^2(y^2+z^2)\right]\right\}dy\,dz +$$

$$\frac{\rho_\infty}{2}\int_{C_2}\chi\frac{\partial}{\partial n}\left[\frac{\lambda}{\rho_\infty U_\infty} f + \frac{\mu}{2\rho_\infty U_\infty}(l-f)^2\right]ds$$

and, by comparison with equations (5b) and (7),

$$D = \frac{\lambda}{2}A - \frac{\mu}{2}V \tag{12}$$

In order to eliminate the Lagrangian multipliers, the solutions of equations (9) or (11) are needed. It is of interest to remark, however, that comparisons with results based upon combined-flow considerations show that for given base area and zero volume λ can be identified with pressure in the combined-flow field and that for given volume and zero base area (closure) μ is the pressure gradient in the combined-flow field (see ref. 2).

APPLICATIONS

Equations (9) or (11) determine the perturbation potential on the rear Mach envelope and thus lead to the evaluation of wave drag in equations (4). Particular applications are studied in this section. First, bodies with base area prescribed along a trailing edge are considered alone. Second, more particular cases of given volume and zero base area are treated. For given base area, it is proper to think of the body as extending downstream from the trailing edge along a cylindrical surface

having elements parallel to the stream direction. A semi-infinite shape then results. If the trailing edge is of supersonic type, all influences downstream of this edge can have no effect on the forward portion of the body and, except for the base drag arising from the unknown pressure at the trailing edge, the wave-drag calculations apply without regard to the cylindrical afterbody.

The two final bodies given here show how, for particular examples, the actual surface shape can be determined from a knowledge of the function χ. Bodies of revolution are chosen for the examples since the integral equations that appear in the analysis involve a single integration. In general, double-integral equations will result and determination of surface shape becomes correspondingly more difficult, if possible at all.

Wings and Bodies Having Given Base Area

The constraint on volume is now removed and the dependence of drag on base area alone is considered. From equation (10), with $\mu = 0$, and equation (4a), drag is

$$D = \frac{\rho_\infty}{2} \iint_S (\Omega_y^2+\Omega_z^2)dy\ dz - \frac{\lambda}{U_\infty} \iint_S (f_y\Omega_y+f_z\Omega_z)dy\ dz +$$

$$\frac{\lambda^2}{2\rho_\infty U_\infty^2} \iint_S (f_y^2+f_z^2)dy\ dz \tag{13}$$

Green's theorem can again be used to rewrite the first two integrals and the last term is simplified by virtue of the relation $f_y^2 + f_z^2 = \beta^2$ In this manner one gets

$$D = -\frac{\rho_\infty}{2} \iint_S \Omega\nabla^2\Omega\ dy\ dz - \frac{\rho_\infty}{2} \int_{C_1+C_2} \Omega \frac{\partial\Omega}{\partial n}\ ds + \frac{\lambda}{U_\infty} \iint_S f\nabla^2\Omega\ dy\ dz +$$

$$\frac{\lambda}{U_\infty} \int_{C_1+C_2} f \frac{\partial\Omega}{\partial n}\ ds + \frac{\lambda^2}{4q_\infty} \beta^2 S$$

where, in the last term, q_∞ is dynamic pressure $\left(= \frac{1}{2} \rho_\infty U_\infty^2\right)$. From equations (11), this relation reduces to

$$D = \frac{\lambda}{2U_\infty} \int_{C_1} \frac{\partial\Omega}{\partial n} f \, ds + \frac{\lambda^2}{4q_\infty} \beta^2 S \tag{14}$$

Further reduction of equation (14) depends on a knowledge of the explicit solution of equations (11). A large and particularly interesting class of wings and bodies for which the solution is immediate is characterized by the condition $f = \text{const.}$ on C_1. Since $x = f(y,z)$ is the equation for the rear Mach envelope, the imposed condition implies that the outer curve Γ_1 of this envelope lies in a plane normal to the stream direction. For example, all wings with plan forms having fore and aft symmetry satisfy this requirement as do also all pointed configurations with subsonic edges so long as the nose and tail vertices determine a line parallel to the stream direction. The solution of equations (11) is then

$$\Omega = \text{const.}$$

and equation (14) reduces to

$$D = \frac{\lambda^2}{4q_\infty} \beta^2 S \tag{15}$$

By means of equations (12) and (15), λ can be eliminated and drag expressed in terms of the geometry of the body or wing. The result is

$$\frac{D}{q_\infty} = \frac{A^2}{(M_\infty{}^2-1)S} \tag{16}$$

The simplicity of equation (16) is remarkable and examples of its rather diverse applicability are given below. Before proceeding to these applications, however, it should be noted that a similar result applies to all planar wings for which the surfaces Σ_1 and Σ_2 intersect along any plane parallel to the z axis. The former condition that the curve Γ_1 lies in a plane normal to the stream is thus relaxed so that $x = f = m(y + b_0)$ on the curve C_1, where $m(<\beta)$ is the slope of the plane of Γ_1 relative to the stream direction. The solution of equations (11) is

$$\Omega = \frac{\lambda m}{\rho_\infty U_\infty} (y+b_0) \qquad \text{in} \quad S$$

and it follows that

$$\frac{\partial\Omega}{\partial n} = \frac{\lambda m}{\rho_\infty U_\infty} \cos(n,y) \qquad \text{on} \quad C_1$$

After substitution of these results into equation (14), one gets

$$D = \frac{\lambda^2}{4q_\infty}(\beta^2-m^2)S \tag{17}$$

In this latter case, therefore, equations (17) and (12) give

$$\frac{D}{q_\infty} = \frac{A^2}{S(\beta^2-m^2)} = \frac{A^2}{(M_\infty{}^2-1-m^2)S} \tag{18}$$

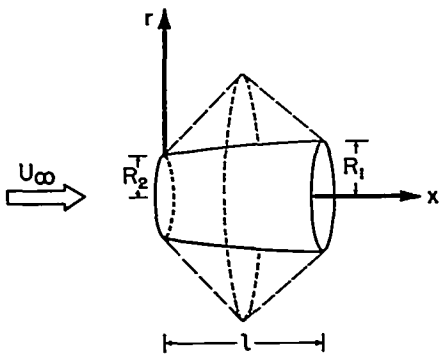

Sketch (c)

Ducted body of revolution with prescribed end diameters.- This problem was first considered by Parker in reference 5. As shown in sketch (c), a shape with minimum external wave drag is constructed so as to have an initial radius R_2 and a final radius R_1. In order that the previous linear theory should apply, the restriction is made that the ratio $\beta|R_1-R_2|/l$ should be a small quantity. If the origin of axes is in the front face of the body, the fore and rear Mach surfaces are

$$x = \beta(r-R_2) \qquad x-l = -\beta(r-R_1)$$

and the curve C_1 is a circle of radius R_o where

$$R_o = (l+\beta R_1+\beta R_2)/2\beta$$

From equation (16) drag is

$$\frac{D}{q_\infty} = \frac{4(R_1{}^2 - R_2{}^2)^2\pi}{(l+\beta R_1+\beta R_2)^2-4\beta^2R_1{}^2} \tag{19a}$$

Equation (19a) is of particular interest since it represents a whole spectrum of results that extends from slender-body theory, for $\beta R_1/l$ and $\beta R_2/l$ small, to two-dimensional theory, for $\beta R_1/l$ and $\beta R_2/l$ large. The slender-body result leads directly to the familiar Kármán ogive formula (ref. 6)

$$\frac{D_K}{q_\infty} = \frac{4A^2}{\pi l^2} \tag{19b}$$

Elliptic plan form with afterbody.- The problem of given base area along the rear edge of an elliptic wing was considered first by R. T. Jones (ref. 3). The figure is a semi-infinite body with a cylindrical shape drawn downstream of the rear edge of an ellipse, see sketch (d). The equation of the plan form outline is assumed to be

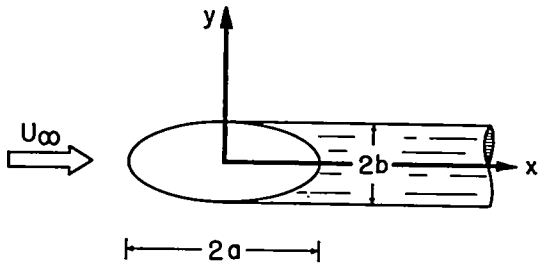

Sketch (d)

$$\frac{x^2}{a^2} + \frac{y^2}{b^2} = 1$$

and the enveloping Mach surfaces are determined completely by the fore and aft Mach cones with vertices along the supersonic-edged portion of the plan form, that is, the abscissas of the vertices lie within the region

$$|x| < a^2/(a^2+b^2\beta^2)^{1/2}$$

The curve C_1 has the equation

$$\frac{y^2}{[(a^2+b^2\beta^2)^{1/2}/\beta]^2} + \frac{z^2}{(a/\beta)^2} = 1$$

and is an ellipse with foci at $(\pm b,0)$. Equation (16) then yields

$$\frac{D}{q_\infty} = \frac{A^2}{\pi a(a^2+b^2\beta^2)^{1/2}} \tag{20a}$$

If drag coefficient C_D is based on plan-form area, equation (20a) can be re-expressed as

$$C_D = \left(\frac{A}{4b^2}\right)^2 \frac{AR^2}{[\beta^2+(4/\pi AR)^2]^{1/2}} \tag{20b}$$

since the aspect ratio of the wing is $AR = (4b)/(\pi a)$. Perhaps the most convenient formula for comparison follows from equations (19b) and (20a) if the drag of the wing is expressed in terms of the drag of a Kármán ogive with the same length and base area. The ratio is given by

$$\frac{D}{D_K} = \frac{a}{(a^2+b^2\beta^2)^{1/2}} = \frac{1}{[1+(\pi\beta AR/4)^2]^{1/2}} \tag{21}$$

The wave drag of the elliptic wing with cylindrical afterbody, in the limit as aspect ratio approaches zero, is equal to the drag of the Kármán ogive and afterbody. For finite values of aspect ratio, the wave drag of the flat wing is smaller than that of the body of revolution, the initial deviation of the ratio from unity being proportional to $(\beta Æ)^2$.

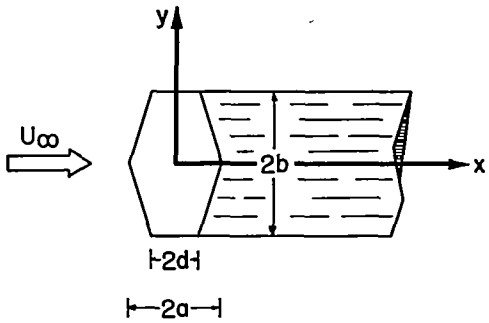

Sketch (e)

Trapezoidal plan form with afterbody.- As a third example, consider a trapezoidal plan form of arbitrary taper ratio with base area along its trailing edge fixed. When the trailing edge is of subsonic type a cylindrical afterbody is assumed added. As shown in sketch (e), root chord is equal to 2a and span equal to 2b. The tip chord is 2d so that taper ratio λ_o and aspect ratio Æ may be introduced in the form

$$\lambda_o = d/a$$

$$Æ = 2b/[a(1+\lambda_o)]$$

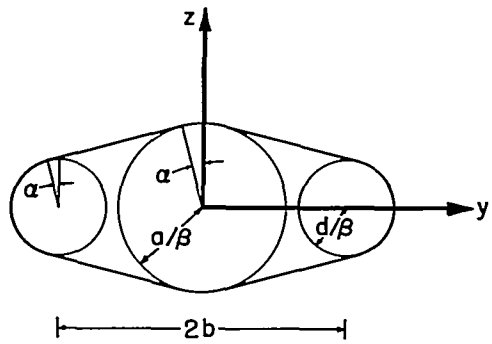

Sketch (f)

So long as the leading edge of the wing is supersonic the characteristic trace C_1 is as shown in sketch (f) and is composed of arcs of circles and straight lines, the radii of the inner and outer circles being a/β and d/β, respectively. The distance between the centers of the two outer circles is 2b. Once the leading edge of the plan form is subsonic, the central circle of sketch (f) blankets the other parts of the figure and C_1 is the circle of radius a/β.

The area S is the sum of elementary geometric areas and is given by

$$S = \frac{2a^2}{\beta^2}\left[\frac{\pi}{2}\lambda_o^2 + \frac{(1+\lambda_o)^2}{2}\beta Æ \cos\alpha + \alpha(1-\lambda_o^2)\right]$$

where α, shown in the sketch, is given by

$$\alpha = \begin{cases} \arcsin \dfrac{2(1-\lambda_o)}{\beta AR\,(1+\lambda_o)}, & 2(1-\lambda_o) \leqq \beta AR\,(1+\lambda_o) \\ \dfrac{\pi}{2}, & 2(1-\lambda_o) \geqq \beta AR\,(1+\lambda_o) \end{cases}$$

From equations (16) and (19b), the minimum drag of the trapezoidal wing relative to the drag of the Kármán ogive of equal length and base area is

$$\left.\begin{aligned} \frac{D}{D_K} &= \frac{\pi}{\pi+(1+\lambda_o)\left[(1+\lambda_o)^2\beta^2 AR^2-4(1-\lambda_o)^2\right]^{1/2}-2(1-\lambda_o^2)\arccos\left[\dfrac{2(1-\lambda_o)}{\beta AR\,(1+\lambda_o)}\right]} \\ &\text{when} \\ &\qquad 2(1-\lambda_o) \leqq \beta AR\,(1+\lambda_o) \\ \frac{D}{D_K} &= 1 \\ &\text{when} \\ &\qquad 2(1-\lambda_o) \geqq \beta AR\,(1+\lambda_o) \end{aligned}\right\} \tag{22}$$

Special cases of interest are:

<u>Rectangular wing</u> ($\lambda_o = 1$)

$$\frac{D}{D_K} = \frac{1}{1 + (4\beta AR)/\pi} \tag{23}$$

<u>Diamond wing</u> ($\lambda_o = 0$)

$$\left.\begin{aligned} \frac{D}{D_K} &= \frac{1}{1 + \dfrac{1}{\pi}\left[(\beta AR)^2 - 4\right]^{1/2} - \dfrac{2}{\pi}\arccos\left(\dfrac{2}{\beta AR}\right)}, \qquad 2 \leqq \beta AR \\ &= 1, \qquad \beta AR \leqq 2 \end{aligned}\right\} \tag{24}$$

Sketch (g) shows a plot of D/D_K against βAR for the elliptic, rectangular, trapezoidal, and diamond plan forms. Base area and length of the wings are equal to these parameters for the Kármán ogive. For large values of βAR the relative drag decreases as $1/\beta AR$. As the wing plan forms become slender, drag of the elliptic and rectangular wings approaches in the limit of vanishing βAR the drag of the ogive. The tapered wing, on the other hand, has a value of drag equal to that of the ogive for all values of taper ratio and aspect ratio satisfying the inequality $2(1-\lambda_o) \geqq \beta AR(1+\lambda_o)$. This relation is satisfied so long as the edges of the wing are subsonic. Changes in sweep angle of the leading and trailing edges produce no further change in the minimum drag of the configuration so long as the base area is held fixed. The value D_K is the minimum drag for all such configurations lying within the fore and aft Mach cones from the nose and tail of the wing. Except in the case of the rectangular plan form, the curves of D/D_K have zero slope at their peak values.

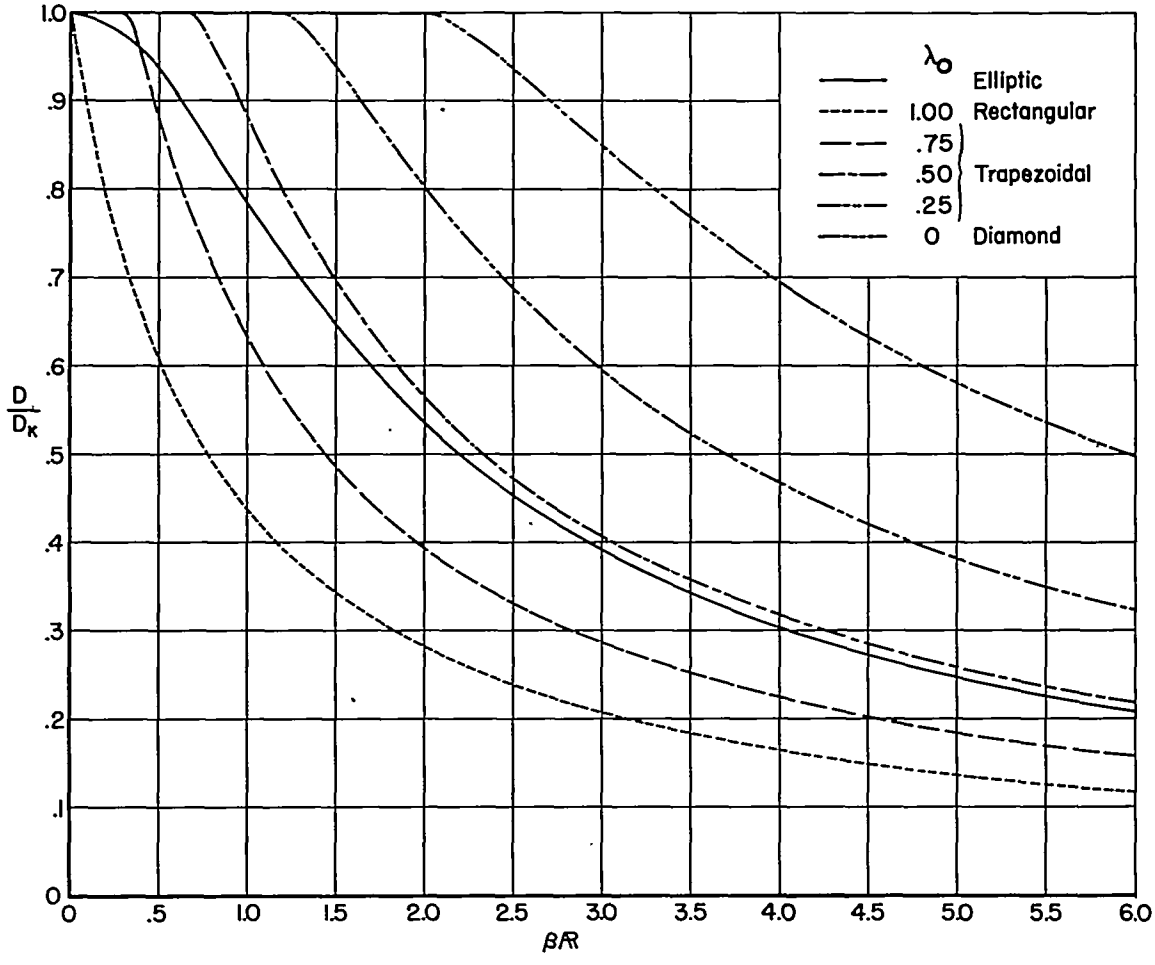

Sketch (g)

It should be noted that among the optimum configurations considered here the Kármán ogive has the greatest value of wave drag for given length, base area, and Mach number. The generality of this observation is apparent from equation (16). Let the family of wings include all plan forms for which the curve Γ_1 lies in a plane normal to the stream direction; the maximum value of minimum drag occurs when S is a minimum and this occurs when the trace C_2 is the circular curve associated with the Kármán ogive of equal length and base area.

Yawed elliptic plan form with afterbody.- For given base area, the drag of an elliptic plan form at angle of yaw ψ can be calculated from equation (18). In order to justify this statement it is sufficient to show that the characteristic curve Γ_1 lies in the plane $x = f = m(y + b_o)$. The trace of Γ_1 in a yz plane is, in fact, another ellipse and the dimensional relationships between the plan form and the trace are as shown in sketch (h). It is convenient in the derivation of these results to proceed inversely and to determine the plan form as an envelope of curves given by the intersections in the xy plane of fore and rear facing cones with vertices on Γ_1. Since the streamwise position of the origin is of no direct significance, the space curve Γ_1 may be assumed given by

$$\left.\begin{aligned} \frac{y^2}{B^2} + \frac{z^2}{C^2} &= 1, \qquad B \geq C \\ x &= my, \qquad m < \beta \end{aligned}\right\} \qquad (25)$$

The Mach cones with vertices at the point (x_1, y_1, z_1) on Γ_1 are

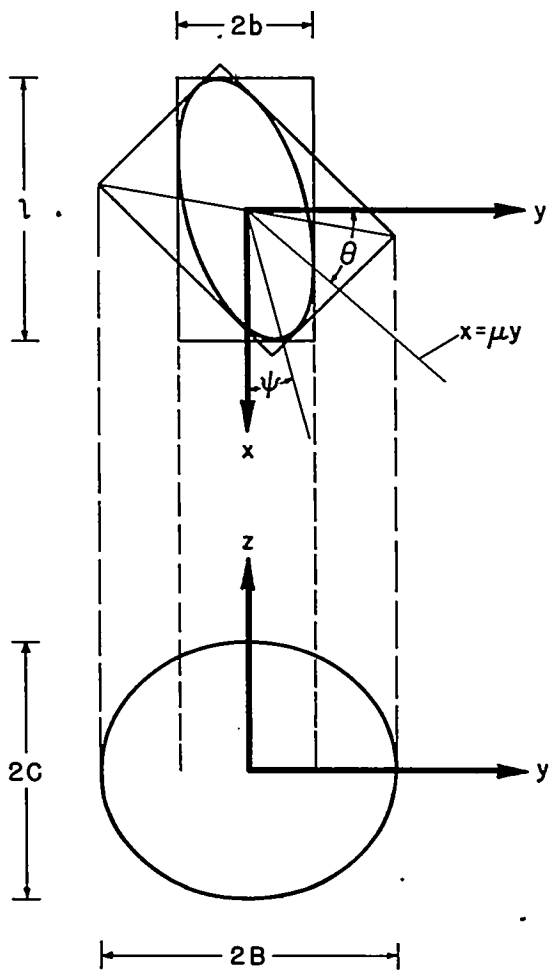

Sketch (h)

$$(x-x_1)^2 = \beta^2[(y-y_1)^2 + (z-z_1)^2] \qquad (26)$$

where

$$x_1 = my_1 , \qquad z_1^2 = \frac{C^2}{B^2}(B^2-y_1^2)$$

The parametric equation of the envelope in the yz plane is given by equation (26) with $z = 0$ and the y_1 derivative of the same expression, that is, the relations

$$B^2[(x-my_1)^2 - \beta^2(y-y_1)^2] = \beta^2C^2(B^2-y_1^2)$$

$$[B^2m^2-\beta^2(B^2-C^2)]y_1 = (mx-\beta^2y)B^2$$

The envelope is, therefore,

$$(B^2-C^2)x^2 - 2mB^2xy + (m^2B^2+\beta^2C^2)y^2 = C^2[\beta^2(B^2-C^2) - m^2B^2] \tag{27}$$

Equation (27) represents an ellipse so long as the initially chosen m satisfies the inequality

$$m^2 < \beta^2(B^2-C^2)/B^2 \tag{28}$$

The elliptical plan form is fixed by its major and minor axes and angle of yaw. The relationship between the plan form and trace curve is more conveniently carried out, however, in terms of the three quantities l, b, μ where l is streamwise length of the plan form, $2b$ its width, and $x = \mu y$ is the line passing through the points on the plan form where $y = \pm b$.

Elementary calculations performed with equation (27) yield the following relations

$$l/2 = (B^2m^2+\beta^2C^2)^{1/2} \tag{29a}$$

$$b = (B^2-C^2)^{1/2} \tag{29b}$$

$$\mu = \frac{mB^2}{B^2-C^2} \tag{29c}$$

$$\tan 2\psi = \frac{-2mB^2}{(B^2-C^2) - (m^2B^2+\beta^2C^2)} \tag{29d}$$

In sketch (h) the plan form is also circumscribed by a parallelogram with sides inclined at the Mach angle. The equations of these lines are

$$x = \beta y \pm (\beta-m)B \qquad x = -\beta y \pm (\beta+m)B$$

from which it follows that their outermost intersection points are at $y = \pm B$ and the line connecting the intersection points is $x = my$.

The above results thus show that the Mach lines circumscribing the plan form can be used to determine the span of the trace of Γ_1 and the angle of inclination of the plane of Γ_1. The span of the plan form is, moreover, equal to the distance between the foci of the elliptic trace.

From equations (18) and (19b) the drag of the wing and afterbody relative to the drag of the Kármán ogive of equal length and base area is given by

$$\frac{D}{D_k} = \frac{l^2}{4BC(\beta^2-m^2)} = \frac{B^2m^2+\beta^2C^2}{BC(\beta^2-m^2)} \tag{30}$$

The results can be summarized as follows

$$\frac{D}{D_K} = \left\{\frac{1+\beta^2\xi^2+[(1+\beta^2\xi^2)^2-4\beta^2\mu^2\xi^4]^{1/2}}{1-\beta^2\xi^2+[(1+\beta^2\xi^2)^2-4\beta^2\mu^2\xi^4]^{1/2}}\right\}^{1/2} \frac{1}{[(1+\beta^2\xi^2)^2-4\beta^2\mu^2\xi^4]^{1/2}} \tag{31}$$

$$AR = \frac{4\xi}{\pi(1-\mu^2\xi^2)^{1/2}}, \qquad \xi = 2b/l \tag{32}$$

$$\tan 2\psi = \frac{2\mu\xi^2}{1-\xi^2} \tag{33}$$

Sketch (i) is a plot of D/D_K against angle of yaw for $M = \sqrt{2}$ and $AR = 4/\pi$, 4, 8. The smallest of these values of aspect ratio corresponds to a circular plan form and obviously must be independent of ψ; the drag ratio is $D/D_K = \sqrt{2}/2$ and this is in agreement with equation (21) for the special case of the circular wing. Several limiting forms of equation (31) are of interest in showing the variation of drag. For example, when $\mu = 0$, the plan form is unyawed, $AR = 4\xi/\pi$ and

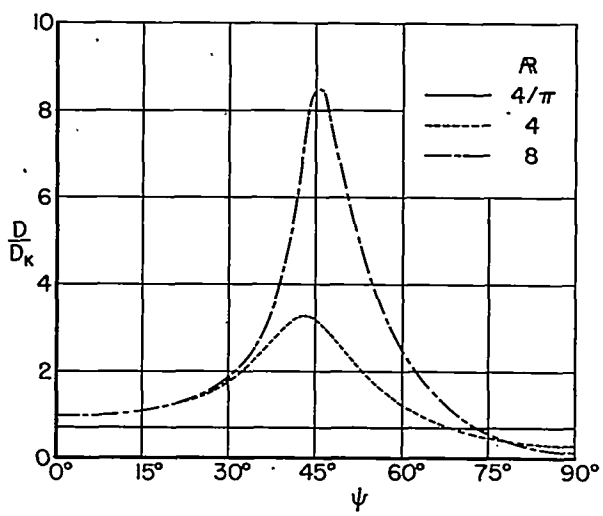

Sketch (i)

$$\frac{D}{D_k} = \frac{1}{(1+\beta^2\xi^2)^{1/2}} = \frac{1}{[1+(\pi\beta AR/4)^2]^{1/2}}$$

as given in equation (21). This relation furnishes the values of D/D_K in sketch (i) at $\psi = 90^\circ$. If $\mu\xi = 1$ and $\xi \neq 0$ one has $AR = \infty$ $\psi = \text{arc tan } \xi$ and

$$\frac{D}{D_k} = \frac{1}{(1-\beta^2\tan^2\psi)^{3/4}}$$

This is the general drag relation for the yawed wing when aspect ratio becomes infinite. It is to be noted that drag remains finite except when the angle of yaw is equal to the free-stream Mach angle. In sketch (i) the drag curve for infinite aspect ratio must therefore have a singularity at $\psi = 45^\circ$. If $\mu\xi \rightarrow 1$ and $\xi \rightarrow 0$ so that aspect ratio remains finite, it follows that $\psi \rightarrow 0$ and $D/D_K = 1$.

Ducted Body of Revolution of Given Volume

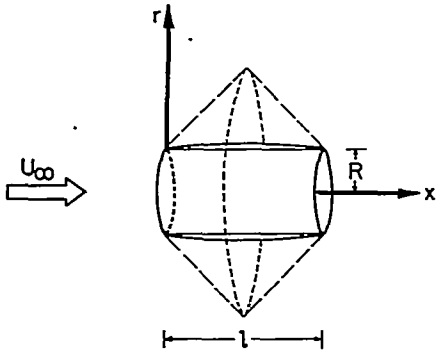

Sketch (j)

External wave drag of a quasi-cylindrical body of revolution is to be minimized, see sketch (j). The radii of the body at the nose and tail are assumed equal (=R) and the volume, V, of the body external to the reference cylinder is a known constant. The value of the minimum drag and, as will be developed in the next section, the evaluation of the body shape can be determined from the solution of equations (11). The equations of the fore and rear Mach envelopes are given respectively by

$$x = \beta(r-R) \qquad x = f = l - \beta(r-R) = \beta(2h+R-r) \tag{34}$$

where the constant h $(=l/2\beta)$ is introduced for convenience. The curve Γ_1 is a circle of radius $r = R + h$ in the plane $x = \beta h$ and equations (11) thus take the form

$$\left.\begin{aligned}
&\nabla^2\Omega = 0 \qquad \text{for} \quad r \leqq R + h \\
&\frac{\partial}{\partial r}\Omega = \frac{\mu\beta^2 R}{2\rho_\infty U_\infty} \qquad \text{at} \quad r = R \\
&\Omega = \frac{\lambda\beta}{\rho_\infty U_\infty} h + \frac{\mu\beta^2}{2\rho_\infty U_\infty}\left[h^2 + \frac{(R+h)^2}{2}\right] \qquad \text{at} \quad r = R + h
\end{aligned}\right\} \tag{35}$$

The solution of equations (35) can be expressed in the form

$$\Omega = k_1 + k_2 \ln[r/(R+h)]$$

where, from the boundary conditions,

$$k_1 = \frac{\lambda\beta}{\rho_\infty U_\infty} h + \frac{\mu\beta^2}{2\rho_\infty U_\infty}\left[h^2 + \frac{(R+h)^2}{2}\right], \qquad k_2 = \frac{\mu\beta^2 R^2}{2\rho_\infty U_\infty}$$

This result, together with equation (10), determines the function χ once the relationship between λ and μ is established from the body closure condition. If the known quantities χ and f are substituted into equation (5b) and A set equal to zero, the desired relation is seen to be

$$\lambda = h\mu\beta \tag{36}$$

and the final form for Ω is

$$\Omega = \frac{\mu\beta^2}{2\rho_\infty U_\infty}\left[3h^2 + \frac{(R+h)^2}{2} + R^2 \ln \frac{r}{R+h}\right] \tag{37}$$

Drag can now be evaluated directly. A parallelism with the derivation following equation (13) can be maintained if equation (4a) is used and the potential is written

$$\chi = \Omega(y,z) - F(y,z) \tag{38}$$

where, from equation (10),

$$F = \frac{\lambda}{\rho_\infty U_\infty} f + \frac{\mu}{2\rho_\infty U_\infty}\left[(l-f)^2 + \frac{1}{2}\beta^2(y^2+z^2)\right] \tag{39}$$

Drag is given by

$$D = \frac{\rho_\infty}{2}\iint_S (\Omega_y{}^2+\Omega_z{}^2)dy\ dz - \rho_\infty\iint_S (F_y\Omega_y+F_z\Omega_z)dy\ dz + \frac{\rho_\infty}{2}\iint_S (F_y{}^2+F_z{}^2)dy\ dz$$

If Green's theorem is used in the first two integral terms, along with the boundary conditions, one has

$$D = \frac{\rho_\infty}{2}\iint_S (F_y{}^2+F_z{}^2)dy\ dz + \frac{\rho_\infty}{2}\int_{C_1} F\ \frac{\partial\Omega}{\partial n}\ ds +$$

$$\frac{\rho_\infty}{2}\int_{C_2} (2F-\Omega)\ \frac{\mu\beta^2}{2\rho_\infty U_\infty}\ \frac{\partial}{\partial n}\ \frac{(y^2+z^2)}{2}\ ds \tag{40}$$

Equation (40) applies in general. For the particular problem of the ducted cylinder, equations (34) and (39) give

$$F = \frac{\mu\beta^2}{2\rho_\infty U_\infty}\left[3h^2 + (R+h-r)^2 + \frac{r^2}{2}\right]$$

and substitution in equation (40) yields

$$D = \frac{\pi}{8}\ \frac{\beta^4\mu^2}{q_\infty}\left\{\frac{h}{4}\ (2R+h)[(R+h)^2 - 3R^2] + R^4 ln\ \frac{R+h}{R}\right\} \tag{41}$$

The multiplier μ can now be eliminated between equation (12), with $A = 0$, and equation (41). The final result assumes a relatively concise form when written as follows

$$\frac{D}{q_\infty} = \frac{V^2}{l^4 C(\sigma)} \tag{42a}$$

where

$$C(\sigma) = \frac{\pi}{128}\left\{(1+4\sigma)[(1+2\sigma)^2 - 12\sigma^2] + 64\sigma^4 \ln \frac{1+2\sigma}{2\sigma}\right\}, \qquad \sigma = \frac{\beta R}{l}$$

As in the case of the quasi-cylinder with given base area, these results cover the entire spectrum of fineness ratios and yield, in their limiting forms, the results of two-dimensional airfoil theory (biconvex section) and slender-body theory. The latter case, which is the Sears-Haack slender body (refs. 7 and 8), corresponds to $\sigma = 0$. Equation (42a) then becomes

$$\frac{D_{S-H}}{q_\infty} = \frac{128V^2}{\pi l^4} \tag{42b}$$

The above problem was considered previously by Heaslet and Fuller (ref. 9) without recourse to the present techniques but, rather, after expressing drag in terms of the source distribution that could be assumed to generate the external shape of the body. In this approach it becomes necessary to find first the source-distribution function, under minimizing conditions, and to calculate drag and volume subsequently. The details of the calculations are thus less direct since the desired quantities are expressed as integrals involving the hyperbolic influence function of the supersonic source. In reference 9, the function $C(\sigma)$ of equation (42a) appeared in the form (in a slightly modified notation)

$$C(\sigma) = \frac{1}{3}\int_0^1 [(\eta+2\sigma)(1-\eta+2\sigma)]^{1/2}[\eta(1-\eta)E-\sigma(1-4\sigma)(K-E)]d\eta \tag{43}$$

where K and E are elliptic integrals of the first and second kind, respectively, of modulus

$$k = \left[\frac{\eta(1-\eta)}{(\eta+2\sigma)(1-\eta+2\sigma)}\right]^{1/2}$$

The immediate advantage of equation (42a) is, of course, the natural advantage provided by any analytic representation with its precise determination of magnitude and rate of change. From a disparate point of view, the equivalence of the two results gives not only a new fundamental identity in the theory of elliptic functions but also indicates a method whereby further identities can be generated. From the standpoint of direct application, however, the results of reference 9 remain unmodified. The calculations that were used to plot the variation of $C(\sigma)$ were found to check to at least four significant figures with the present formula and thus provided a satisfying confirmation of the numerical techniques used in the original evaluation.

Determination of Surface Shape

In the calculation of minimum drag for the two families of ducted bodies, the value of the perturbation potential on the rear Mach envelope becomes available in explicit form. It is therefore possible to seek the source distribution function $B(x)$ generating the disturbance field on the rear surface; once $B(x)$ is known the body shape can be calculated as the final step in the analysis of the minimum drag bodies. When the source distribution is confined to a single line segment, $B(x)$ appears as the solution of a single-integral equation. The origin is conveniently moved to the starting point of the source distribution ($x = -\beta R$ of sketch (h)), so that $B(0) = 0$. For bodies of revolution, the perturbation potential is known to be given by

$$\varphi(x,r) = \frac{-1}{2\pi}\int_0^{x-\beta r} \frac{B(x_1)dx_1}{[(x-x_1)^2 - \beta^2 r^2]^{1/2}} \tag{44}$$

Since $B(0) = 0$, differentiation and integration by parts yields

$$-\beta\varphi_x + \varphi_r = \frac{1}{2\pi r}\int_0^{x-\beta r} \left[\frac{x+\beta r-x_1}{x-\beta r-x_1}\right]^{1/2} B'(x_1)dx_1$$

where the prime denotes differentiation. The rear surface is

$$x = f = l + 2\beta R - \beta r$$

and on this surface

$$X_r = -\beta\varphi_x + \varphi_r$$

Hence, the integral equation

$$2\pi r X_r = \int_0^{l+2\beta R-2\beta r} \left[\frac{l+2\beta R-x_1}{l+2\beta R-2\beta r-x_1}\right]^{1/2} B'(x_1)dx_1 \tag{45}$$

results where $2\pi r X_r$ can be assumed known. The transformations

$$\left.\begin{aligned} t &= l+2\beta R-2\beta r \\ G(x) &= (l+2\beta R-x)^{1/2}B'(x) \\ H(t) &= 2\pi r X_r(r) \end{aligned}\right\} \tag{46}$$

lead to the Abel type equation

$$H(t) = \int_0^t \frac{G(x_1)dx_1}{(t-x_1)^{1/2}} \tag{47}$$

and its solution is known to be

$$G(t) = \frac{1}{\pi}\frac{d}{dt}\int_0^t \frac{H(t_1)dt_1}{(t-t_1)^{1/2}} \tag{48}$$

For the case of given base area ($\mu = 0$), the solution of equations (11) was Ω = const., hence, from equation (10)

$$X = -\frac{\lambda}{\rho_\infty U_\infty} f + \text{const.}$$

and

$$X_r = \frac{\lambda\beta}{\rho_\infty U_\infty}$$

From equations (12) and (15) it follows that

$$\lambda = \frac{2q_\infty A}{\beta^2 S}$$

so that one has

$$H(t) = \frac{U_\infty \pi A}{\beta^2 S}(l+2\beta R-t)$$

Substitution into equation (48) yields $G(t)$ and from equations (46) the source distribution functions (with x as in sketch (h))

$$\left.\begin{aligned} B'(x) &= \frac{U_\infty A}{\beta^2 S}\,\frac{l-2x}{[(x+\beta R)(l+\beta R-x)]^{1/2}} \\ B(x) &= \frac{2U_\infty A}{\beta^2 S}\,[(x+\beta R)(l+\beta R-x)]^{1/2} \end{aligned}\right\} \tag{49}$$

For the case of given volume, equations (37), (38), and (39) yield

$$rX_r = \frac{\mu\beta^2}{2\rho_\infty U_\infty}\,[R^2 + 2(R+h)r - 3r^2]$$

and the determination of the source distribution function follows directly. The final form of this function is

$$B(x) = \frac{U_\infty V}{2l^4 C(\sigma)}\left\{(l-2x)[(x+\beta R)(l+\beta R-x)]^{1/2} - 2\beta^2R^2 \operatorname{arc\,cos}\frac{l-2x}{l+2\beta R}\right\} \tag{50}$$

The geometries of the two families of bodies were calculated and shown in reference 9 and will not be repeated here. Comparable results to those of sketch (g) are, however, given in sketch (k). For the case of given volume, the drag of the quasi-cylinders relative to that of the Sears-Haack slender body is, from equations (42a) and (42b),

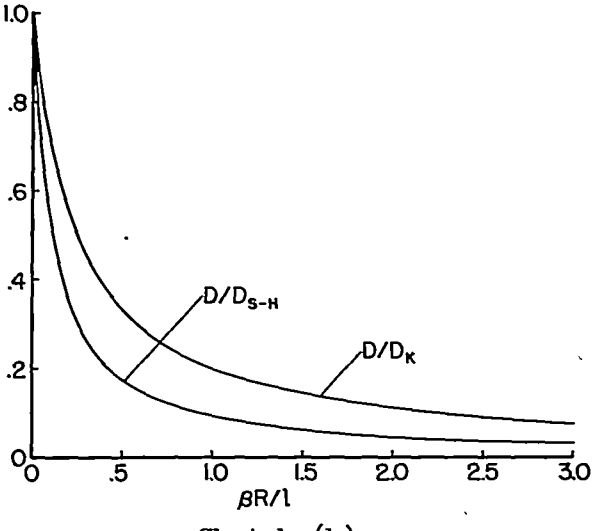

Sketch (k)

$$\frac{D}{D_{S-H}} = \frac{\pi}{128C(\sigma)} \tag{51}$$

For the case of given base area the drag formula is reduced to the form it would take in reference surface theory. Under the assumption that R_2 deviates slightly from R_1, equations (19a) and (19b) yield

$$\frac{D}{D_K} = \frac{1}{1+4\sigma} \tag{52}$$

CONCLUDING REMARKS

As given by equation (4a), drag is equal to the kinetic energy in a two-dimensional flow field of unit thickness. Intuitively, the results are remindful of the similar expression for the vortex drag of a lifting wing in subsonic flow theory. In this latter Trefftz plane analysis, the optimum field is represented by a harmonic function in the entire cross-flow plane external to the trace of the body whereas, in supersonic flow, an additional, outer, bounding curve C_1 appears and affects the induced velocities and the wave drag. The flow field associated with minimum drag due to lift remains a harmonic field on the rear Mach envelope in supersonic flow (ref. 1) and, as shown in the present paper, the flow in the nonlifting case is also a harmonic field with known additional effects. Another point of similarity between the subsonic and supersonic theories also appears: the boundary conditions determining the induced field are given along curves that are uniquely determined by the wing or body but the details of plan-form shape are not determined uniquely from the bounding conditions themselves. Thus, in Prandtl's and Munk's vortex theory, the flow in the Trefftz plane can be calculated but the chordwise dimension of the wing disappears entirely; all wings with equal span have the same minimum drag and the same spanwise distribution of loading for minimum drag. It is obviously impossible to solve for details of the chordwise load distribution in this case. In supersonic theory the conditions for minimum drag are given on a surface displaced from the body and a loss in knowledge as to plan-form shape is thus incurred. In the case of the trapezoidal plan forms with given base area, minimum drag and induced velocities on the Mach envelope remain fixed for the entire family of wings with subsonic leading and trailing edges. The solution of the problem allowed for no storage of information about taper ratio and aspect ratio once the wing was swept behind the Mach cone from the vertex. There remains the final question, however, as to whether a multiplicity of solutions can be found. Suppose a planar wing exists and consider the shape equal to the difference between the wing and the Kármán ogive. From equation (14) the drag of the latter shape is zero. But for nonvanishing thickness, wave drag can never be zero. The logical contradiction implies that the Kármán ogive is the only minimum drag configuration within the family of trapezoidal plan forms with subsonic edges.

Following equation (12) it was remarked that the parameter λ could be identified with pressure in the combined flow field. An interesting interpretation of the value of this parameter follows from the use of equation (15). Eliminating drag between the two relations, one gets

$$\frac{\lambda}{2q_\infty} = \frac{A}{\beta^2 S} \tag{53}$$

The left-hand expression is half of pressure coefficient in the combined flow field. Equation (53) states that the value of $-\lambda/q_\infty$ necessary to calculate minimum drag is equal to the pressure coefficient predicted by linearized unidimensional flow theory in a duct bounded internally and externally by the characteristic traces, that is, the curves C_1 and C_2 of sketch (b).

Ames Aeronautical Laboratory
National Advisory Committee for Aeronautics
Moffett Field, Calif., June 24, 1957

REFERENCES

1. Ward, G. N.: On the Minimum Drag of Thin Lifting Bodies in Steady Supersonic Flows. British A.R.C. Rep. 18,711, FM 2459, 1956.

2. Jones, Robert T.: The Minimum Drag of Thin Wings in Frictionless Flow. Jour. Aero. Sci., vol. 18, no. 2., Feb. 1951, pp. 75-81.

3. Jones, Robert T.: Theoretical Determination of the Minimum Drag of Airfoils at Supersonic Speeds. Jour. Aero. Sci., vol. 19, no. 12, 1952, pp. 813-822.

4. Heaslet, Max. A., and Lomax, Harvard: Supersonic and Transonic Small Perturbation Theory. Sec. D of General Theory of High Speed Aerodynamics. Vol. VI of High Speed Aerodynamics and Jet Propulsion, W. R. Sears, ed., Princeton Univ. Press, 1954, pp. 122-344.

5. Parker, Hermon M.: Minimum-Drag Ducted and Pointed Bodies of Revolution Based on Linearized Supersonic Theory. NACA Rep. 1213, 1955. (Supersedes NACA TN 3189.)

6. von Kármán, Th.: The Problem of Resistance in Compressible Fluids. Proc. Fifth Volta Congress, Rome, Sept. 30 - Oct. 6, 1935. (Also available as GALCIT Pub. 75.)

7. Sears, William R.: On Projectiles of Minimum Wave Drag. Quart. Appl. Math., vol. IV, no. 4, Jan. 1947, pp. 361-366.

8. Haack, W.: Geschossformen kleinsten Wellen-widerstandes. Lilienthal-Gesellschaft fur Luftfahrtforschung, Bericht 139, Teil 1, Oct. 9-10, 1941, pp. 14-28.

9. Heaslet, Max. A., and Fuller, Franklyn B.: Axially Symmetric Shapes With Minimum Wave Drag. NACA Rep. 1256, 1956. (Supersedes NACA TN 3389.)

NACA - Langley Field, Va.